

Improved P3HT:PCBM photovoltaic cells with two-fold stabilized PbS nanoparticles

J. L. ALONSO*, J. C. FERRER, F. RODRÍGUEZ-MAS, S. FERNÁNDEZ DE ÁVILA

Universidad Miguel Hernández, Communications Engineering Department, Av. Universidad, s/n, Ed. Innova, 03202, Elche, Spain

Lead sulfide nanoparticles have been synthesized by a simple, low-temperature method, using thiophenol and decanethiol as stabilizing agents. Transmission electron microscopy characterization shows nanocrystals with an average size of 4.5 nm. Optical absorption spectroscopy suggests that strong quantum confinement of charge carriers has been achieved. The nanoparticles have been easily incorporated into a poly(3-hexylthiophene):phenyl-C61-butyric acid methyl ester in chlorobenzene solution. A photovoltaic cell has been fabricated using this mixture as active layer and compared to a reference cell without nanoparticles. Electrical measurements show a significant improvement of the electrical characteristics of the photovoltaic cell based on the hybrid material.

(Received October 29, 2015; accepted September 29, 2016)

Keywords: Nanoparticles, Quantum dots, PbS, Polymer devices, Solar cells

1. Introduction

Photovoltaic cells based on bulk heterojunctions of semiconducting polymers have focused the attention of researchers due to several potential advantages over their inorganic counterparts [1]. The technology employed for the manufacturing of polymer-based devices is attractive because of its simplicity, low cost and ability to process large-area devices even on flexible substrates. Among the different candidates to be used as active material in photovoltaic cells, the mixture of poly(3-hexylthiophene) (P3HT) and phenyl-C61-butyric acid methyl ester (PCBM) has been probably the most extensively studied system. P3HT is a solution processable semiconducting polymer well known for its interesting electrical properties: high mobility of holes ranging from $1.33 \times 10^{-5} \text{ cm}^2 \text{ V}^{-1} \text{ s}^{-1}$ and $3.30 \times 10^{-4} \text{ cm}^2 \text{ V}^{-1} \text{ s}^{-1}$ depending on the molecular weight [2] and low width of the bandgap (1.9 eV) [3]. PCBM is a fullerene derivative commonly used as electron acceptor material in blends with P3HT or other semiconducting polymers [4,5].

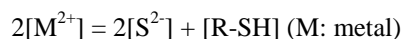
However, the inclusion of low-dimensional inorganic semiconductors in photovoltaic cells may be desirable [6]. Nanometer-sized semiconductor particles, or quantum dots, exhibit interesting properties due to quantum confinement, such as multiple exciton generation [7] or extended optical absorption bands [8], which may help to improve the efficiency of photovoltaic cells. Quantum dots intended for integration in organic devices are commonly synthesized by chemical routes which result in colloidal solutions of nanocrystals [9]. In this case, nanoparticles are capped with organic radicals, bonded to the surface, which play several roles: (i) During reaction of precursors and after formation of the nanoparticles the ligands act as stabilizers preventing the nanoparticles to collapse into

bulk material by Ostwald ripening [10], and are responsible for the size of the nanoparticles as explained later in this section. (ii) The solubility of the nanoparticles when introduced in a solvent depends on the interaction of the nanoparticles surface atoms with the solvent molecules. Thus, adequately choosing the organic radical for the capping layer, nanoparticles based on the same core material can be solubilized in mediums with different polarities. (iii) For quantum dots that are intended to be used in optoelectronic devices such as nanoparticle-doped organic light-emitting diodes or photovoltaic cells, the capping layer plays a critical role in the electrical characteristics of the devices since charge transfer between the quantum dots and the surrounding medium is affected by the band alignment and length of the ligands. This has led to several works focused on ligand exchange of the capping layer in order to improve the performance of optoelectronic devices in which the quantum dots are part of the active layers [11].

Decanethiol and thiophenol are organic radicals commonly used to stabilize quantum dots. However, the properties of nanoparticles differ depending on which radical is employed to cap the surface. Decanethiol is composed by a long carbon chain that solubilizes the nanoparticles in solvents like toluene or chlorobenzene. Thus, since both P3HT and PCBM are soluble in chlorobenzene, nanoparticles capped with this ligand may be solubilized along with these polymers with no risk of undergoing agglomerated or precipitated. However, poor charge transfer through the surface of the quantum dots is expected since the isolating carbon chain is significantly long. On the contrary, thiophenol is a short ligand with delocalized electrons. However, quantum dots capped with this ligand are soluble in dimethyl sulfoxide, which is an unsuitable solvent for the considered polymers.

In this work, PbS quantum dots have been synthesized by a simple method using a mixture of thiophenol and decanethiol as capping agents. The resulting nanoparticles in colloidal suspension in chlorobenzene have been mixed with a P3HT:PCBM polymer solution. The aim of this work is to present a simple method to synthesize PbS nanoparticles with two different stabilizers as well as to prove the improvement of the electrical characteristics of photovoltaic cells based on P3HT:PCBM blend when these PbS nanoparticles are included in the active layer.

The method of preparation of quantum dots capped with thiol radicals used in this work is based on the paper of Herron et al. [10] to synthesize CdS nanoparticles. In the work of Herron, CdS nanoparticles were synthesized by reaction of the metal precursor and two sources of chalcogen: a sulfur salt that provides for the sulfur atoms in the core of the quantum dot, and a thiol that supplies the sulfur atoms that will be bonded to the surface. Since the number of atoms at the surface of a nanoparticle is comparable to the number of atoms at the core, the size of the nanoparticles can be easily controlled by adjusting the molar ratio between the two types of sulfur precursors as follows:

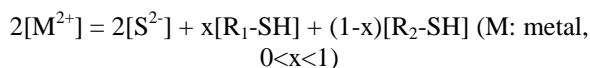


Thus, the size of the nanocrystals increases as the $[S^{2-}]:[R-SH]$ ratio is raised, ranging from pure metal thiolate when $[S^{2-}] = 0$ to bulk semiconductor when concentration of S^{2-} reaches certain limits [12].

One of the difficulties to be addressed when trying to fabricate solution-based polymer-nanoparticle hybrid devices is that solvent suitable for the polymer differs from the solvent in which the colloidal nanoparticles reside. The nanoparticles solvent may be different since they should be capped with organic radicals that are suitable for the charge transfer processes between the nanoparticle and the surrounding matrix.

Thus, a mixture of two types of solvents in several proportions should be used to spin cast the active layer of the devices. That could lead to some shifts of the I-V curves or odd behaviour of the devices as it has previously been reported in [13]. In the former the influence of the solvent used in the fabrication process was proved.

Instead of using a mixture of two solvents, nanoparticles may be capped with two different organic radicals: a radical (R_1) which solubilizes the nanoparticles in the same solvent used to spin-cast the polymer and other radical (R_2) which allows the charge transfer between the nanoparticle and the polymer matrix. In order to obtain such hybrid capping the original balance equation should be modified, taking into account the molar ratio between the two types of capping radicals R_1 and R_2 :



PbS nanoparticles having a mixture of thiophenol and decanethiol surfactants could be a route to avoid the use of two different solvents while presenting both advantages:

good solubility due to decanethiol and charge transfer through thiophenol capping agents.

In order to test the usefulness of dual capped PbS quantum dots, two different photovoltaic solar cells have been fabricated. Performance of solar cells having PbS nanoparticles embedded in P3HT:PCBM matrix has been compared to that of blend P3HT:PCBM reference devices.

2. Materials and methods

2.1. Synthesis of nanoparticles

All reagents were purchased from Sigma-Aldrich and were used without further purification. The selected reagents are all soluble in water/methanol mixtures. $Pb(NO_3)_2$ salt was used as metal precursor. $Na_2S \cdot 9H_2O$ was selected to provide for the core sulfur atoms. Thiophenol, $SH-C_6H_5$, and decanethiol, $SH-C_{10}H_{21}$, were used as capping radicals. A $[S^{2-}]:[SH-R] = 1:10$ molar ratio of core to surface sulfur atoms was chosen. This ratio was based on previous experiments in order to obtain nanoparticles of an average diameter of 4.5 nm [12]. A $[Thiophenol]:[Decanethiol] = 1:4$ molar ratio was selected in order to guarantee the solubility of PbS nanoparticles in chlorobenzene. Following the work of Herron [10], two solutions were prepared. The weights of precursors were calculated to obtain 1 mmol of PbS nanocrystals and were prepared as follows: 331 mg of $Pb(NO_3)_2$ were dissolved in a 5 ml water and 5 ml methanol (solution A); 13 mg of Na_2S , 43 μ l of thiophenol and 265 μ l of decanethiol were dissolved in 5 ml water and 5 ml methanol (solution B). Both solutions were agitated at room temperature during 30 minutes with a stir bar. Then, solution A was added slowly under continuous agitation to solution B resulting in a precipitate that was washed with methanol, centrifuged three times, and dried in a vacuum oven. The resulting nanoparticles were soluble in chlorobenzene.

2.2. Structural and optical characterization of nanoparticles

The PbS nanocrystals were analyzed by transmission electron microscopy (TEM) and UV-visible absorption spectroscopy. TEM images were obtained with a JEOL 2010 microscope operating at 200 kV. Samples for TEM were prepared by deposition of a single drop of the quantum dot solution in chlorobenzene on a 300 mesh copper grid with a carbon supporting film, over a filter paper which absorbed excess solution. The copper grid with the quantum dots was allowed to dry at room temperature. Optical absorption measurements were performed with a T92+ UV/VIS spectrophotometer from PG instruments Ltd.

2.3. Devices fabrication

The structure of the devices is as follows: Glass/ITO/PEDOT:PSS/ACTIVE LAYER/Al. They were

fabricated starting with polished glass substrate coated with a thin (60 nm) semitransparent indium-tin oxide (ITO) layer (2.5 cm × 2.5 cm) of a resistivity of 60 Ohms cm, which will act as the anode of the devices. These substrates were put under a cleaning procedure consisting in dipping the substrates in a NaOH 10% aqueous solution in an ultrasonic bath for three minutes at a temperature of 55 °C. Then, they were rinsed with abundant deionized water for one minute approximately. Finally, they were dried by blowing N₂ onto the surface.

Poly(3,4-ethylenedioxythiophene):poly(styrenesulfonate) (PEDOT:PSS) was used in all devices as hole transporting layer. It was spin coated at 6,000 r.p.m. onto the ITO substrate reaching a thickness of about 75 nm from a 1.3 % PEDOT:PSS water solution (Sigma-Aldrich, grade electronic applications). Then, the layer was cured on a hot plate for an hour at 100 °C in order to enhance the evaporation of the solvent. This layer accomplishes two different goals, on one hand, it enhances the transport of holes from the active layer to the ITO anode, and on the other hand, it prevents the spikes of the ITO layer due to its rugosity touch the aluminium cathode and short-circuit the device.

To perform the active layers two starting solutions were prepared. Solution C consisting in 40.0 mg/ml of P3HT:PCBM (ratio 1:1 by mass) in chlorobenzene and solution D consisting in 40.0 mg/ml of PbS in chlorobenzene. After filtering solution C through a 0.45 µm porous size filter an aliquot of 0.30 ml was extracted and then added 0.90 ml of chlorobenzene resulting in a 10.0 mg/ml solution of P3HT:PCBM (ratio 1:1 by mass) in chlorobenzene. 0.30 ml of this solution were used to spin cast the active layer of the REF-CELL, enough to cover all the surface of the substrate (2.5 cm × 2.5 cm). The spinning velocity was adjusted to 500 r.p.m. in order to achieve the optimum thickness of the layer. Then, it was cured on a hot plate for an hour at 80 °C in order to enhance the evaporation of the solvent. All the products were purchased from Sigma-Aldrich.

Other aliquot of 0.30 ml was extracted from the filtered solution C. Then was added 0.10 ml of solution D and finally 0.80 ml of chlorobenzene. This gave us 1.20 ml of a chlorobenzene solution containing 12.0 mg of P3HT:PCBM and 4.0 mg of PbS. 0.30 ml of this mixture was taken to spin cast de active layer of the PbS-CELL, using identical spinning and curing conditions than our reference solar cell.

It is relevant to note that both solutions used to spin cast the active layer have identical final concentration of P3HT:PCBM in chlorobenzene (10.0 mg/ml) in order to establish good comparison between the two solar cells. This is crucial because it is fully known that the thickness of the layer depends on the concentration and therefore, so does the solar cell behaviour [14].

Finally, metallization of the devices was carried out employing aluminium through mask using Joule effect method in a Univex Oerlikon high vacuum chamber (10⁻⁶ mmHg). The thicknesses reached were about 200 nm. After that, both cells were put through an annealing ramp process. Once the maximum temperature of 120 °C was

achieved, it was kept during two minutes and then it was let cool at room temperature. The solar cells active size was 2 cm × 2 cm.

2.4. Devices characterization methods

A Keithley 2400 Sourcemeeter equipment was used to perform the electronic characterization of the solar cells in darkness and under light conditions. With the aim of avoiding the degradation of the polymeric samples, a pulsed voltage sweep was programmed via LabVIEW in order to control the duty cycle (0.7 %). Light conditions of one Sun (100 mW/cm², AM1.5G, 25 °C) were guaranteed by means of a Newport Solar Simulator consisting of a Xenon Arc lamp and AM1.5G filter and reference calibrated solar cell also from Newport (91150V). The Oriel model 91150V consists of a readout device and a 2 × 2 cm² calibrated solar cell made of monocrystalline silicon. The cell is also equipped with a thermocouple assembled in accordance with IEC 60904-2. The certification is accredited by NIST to the ISO-17025 standard and is traceable both to the National Renewable Energy Laboratory (NREL), and to the International System of Units (SI). It reads solar simulator irradiance in "sun" units.

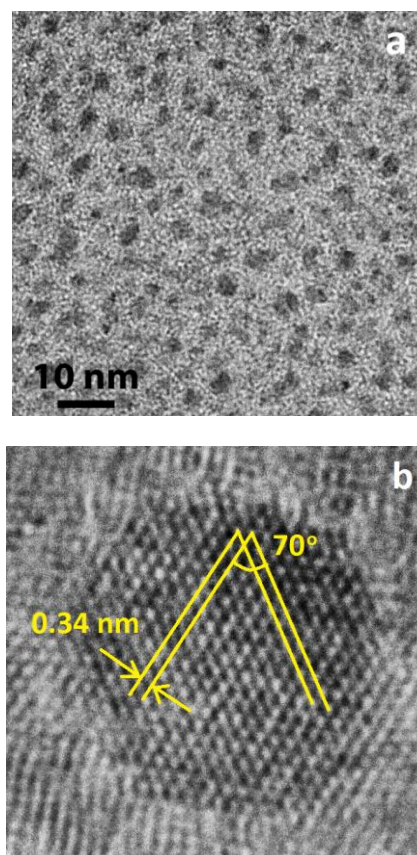


Fig. 1. TEM images of PbS nanocrystals showing homogeneous size and distribution (a) and a single nanoparticle of cubic PbS (b).

3. Results and discussions

3.1. Transmission electron microscopy

Fig. 1a shows a high resolution TEM image of a PbS nanoparticle collection on the amorphous carbon film. Nanocrystals are evenly distributed, without agglomerations. The size of quantum dots have been measured directly on TEM images and an average diameter of 4.5 nm has been obtained. Since the Bohr exciton radius of PbS is 20 nm [15], strong quantum confinement of charge carriers is expected for these nanoparticles

A closer inspection of the nanoparticles allows verifying their composition by measuring the distances and angles between atomic planes. The Fig. 1b shows a high resolution image of a representative single nanoparticle in which the atomic rows are clearly visible. The distance and the angle between nearest neighbor rows are 0.34 nm and 70° respectively, which match the theoretical values of $\{111\}$ planes of cubic PbS observed from a $\langle 110 \rangle$ zone axis.

3.2. Optical absorption

Absorbance measurements were recorded after dispersion of nanocrystals in chlorobenzene using plain chlorobenzene as background signal. The spectrum of the solution, presented in Fig. 2, shows a long tail that could be due to defect states, particle size distribution or indirect transitions. The presence of this tail makes the precise determination of the band gap energy difficult, however, a rough estimation of this parameter from the absorption curve gives an effective bandgap $E_g^* \sim 3.25$ eV, which is far from the bandgap energy of bulk PbS, $E_g = 0.41$ eV [15]. This blue-shift may be explained as the consequence of the apparent difference between the Bohr exciton radius and the size of the nanoparticles found in the previous section. In the same figure is also presented the absorption spectrum of P3HT-PCBM in order to compare the absorption bands of the two phases.

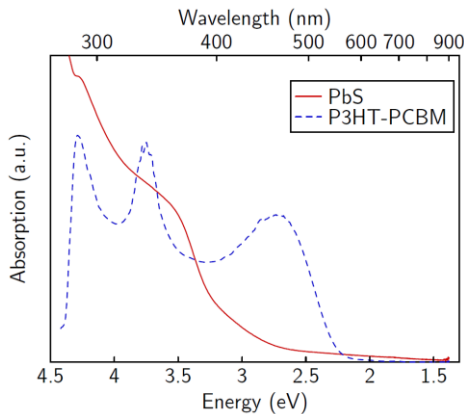


Fig. 2. Optical absorption spectrum of the PbS nanoparticles (red) and P3HT-PCBM (blue) dissolved in chlorobenzene. Absorption edge of PbS nanoparticles is blue-shifted compared to bulk PbS due to quantum confinement

3.3. Electronic characterization of the solar cells

Two different active layers have been assayed, resulting in two different solar cells. One of them was based on the widely known donor-acceptor blend P3HT:PCBM. The solar cell based on this blend will be used as a reference cell, from now on, (REF-CELL). In order to establish comparisons, other active layer was used based on the former blend mixed with PbS quantum dots synthesized like explained below. The solar cell based on this active layer will be named from now on as (PbS-CELL). One of the advantages of using PbS nanoparticles arises on the fact that they have a broad absorbance spectra and a large excitonic radius, which allows to modulate the absorption edge from 3200 nm for the bulk, to 530 nm for very small clusters. Therefore, it is expected the nanoparticles harvest the infrared part of the solar spectrum where the polymeric blend is blind.

The electronic characterization of the solar cells has been carried out as it can be seen in Fig. 3. Particularly, Fig 3.a. shows the current versus voltage curve in darkness conditions and under illumination conditions of one Sun (100 mW/cm^2 , AM1.5G, 25°C) for the reference solar cell based on P3HT:PCBM. The analogous for the PbS-CELL based on P3HT:PCBM:PbS can be seen in Fig. 3.b. The comparison of the I-V curves of the two solar cells under illumination conditions of 1 Sun is established in Fig. 3.c. Furthermore, the power generated by the two solar cells is given in Fig. 3.d.

I-V curves were measured directly whereas the generated power curves were obtained indirectly as the product of the current and the voltage recorded. Typical characterization parameters of a solar cell like short circuit current, I_{sc} , open circuit voltage, V_{oc} , were read directly from the experimental data, while others like the fill factor, FF , or the efficiency, η , were calculated from the experimental data as follows:

$$FF = \frac{V_{MPP} I_{MPP}}{V_{OC} I_{SC}} \quad (1)$$

Where V_{MPP} and I_{MPP} represents the voltage and the current respectively of the point of the I-V curve where the cell delivers maximum power and is generally denoted as the *Maximum Power Point*. The power conversion efficiency, or simply, the efficiency is defined as follows:

$$\eta = \frac{P_{OUT}}{P_{IN}} = \frac{V_{MPP} I_{MPP}}{P_{IN}} = \frac{I_{SC} V_{OC} FF}{P_{IN}} \quad (2)$$

Where P_{IN} stands for the illumination power radiation seen by the cell. Due to our solar cells had an active area of $2 \text{ cm} \times 2 \text{ cm}$ and were illuminated under 1 Sun conditions, the resultant incident light power was 0.40 W. The former parameters and its percentage comparison are summarized in Table 1.

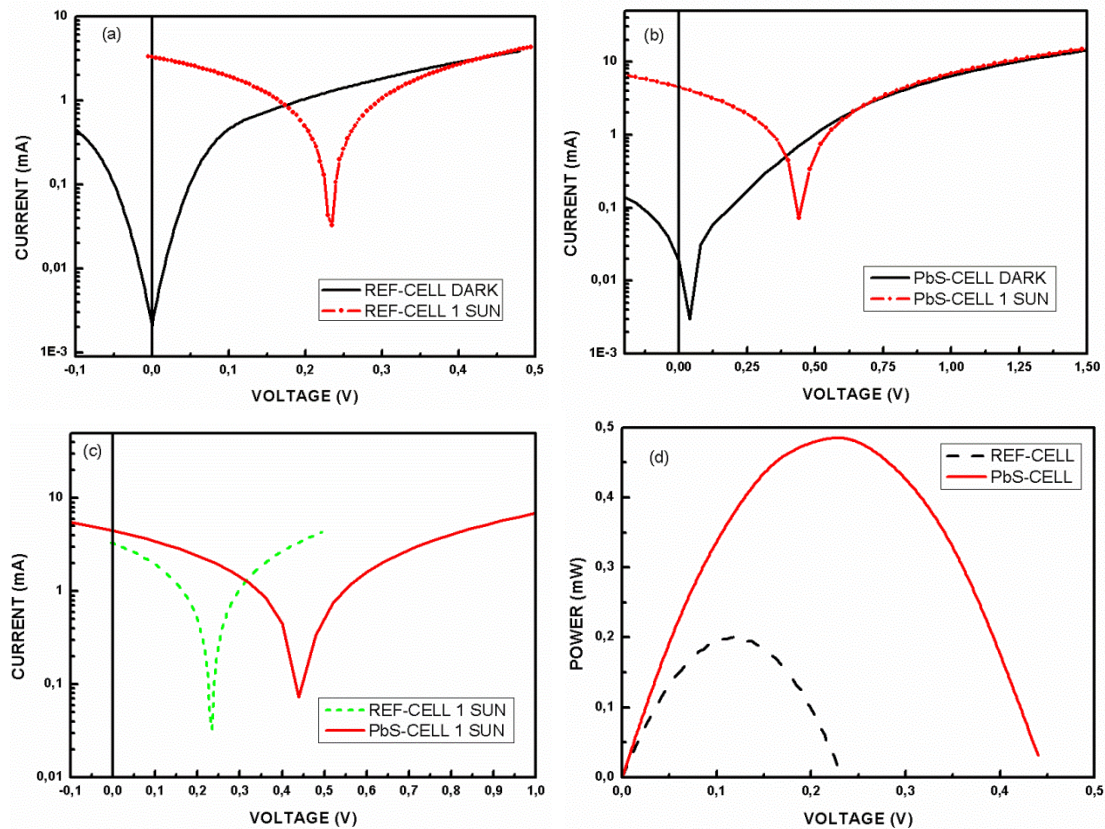


Fig. 3. Electronic characterization of the solar cells. (a) Current versus voltage curve in darkness conditions and under illumination conditions of one Sun (100 mW/cm^2 , AM1.5G, 25°C) for the reference solar cell based on P3HT:PCBM. (b) Current versus voltage curve in darkness conditions and under illumination conditions of one Sun (100 mW/cm^2 , AM1.5G, 25°C) for the hybrid solar cell based on P3HT:PCBM and PbS nanoparticles. (c) Comparison of the I-V curves of the two solar cells under illumination conditions of 1 Sun. (d) Power generated by the REF-CELL and the PbS-CELL

Table 1. Summary of the electronic parameters and its compared improvements for the REF-CELL and the PbS-CELL solar cells

| CELL | ACTIVE LAYER | Short-circuit current I_{sc} (mA) | Open Circuit Voltage V_{oc} (V) | Maximum Power Point MPP (mW) | Fill Factor FF (%) | Power Efficiency η (%) |
|-----------------|---------------|--|--------------------------------------|---------------------------------|-----------------------|--------------------------------|
| REF-CELL | P3HT:PCBM | 3.30 | 0.23 | 0.20 | 26.32 | 0.05 |
| PbS-CELL | P3HT:PCBM:PbS | 4.50 | 0.48 | 0.49 | 22.70 | 0.12 |
| IMPROVEMENT (%) | | 36.36 | 108.70 | 145.00 | -13.75 | 140.00 |

In view of the results obtained, the solar cell made up of hybrid materials -polymeric blend and PbS quantum dots- experiments a significant improvement compared to that without PbS nanoparticles. All the electronic parameters suffer a relevant increase except the fill factor that is nearly the same.

In particular, the short circuit current of the PbS-CELL is considerable greater than the one of REF-CELL, it goes from 3.30 mA to 4.50 mA. This means an

improvement of this crucial parameter of 36.36 %. Remarkably, the open circuit voltage of the hybrid cell suffers even a greater increase passing from 0.23 V to 0.48 V. Achieving in this case an improvement of 108.70 %. Concerning the maximum power point, it is not at all negligible the advantages showed by the PbS-CELL. The device increases its value from 0.20 mW to 0.49 mW, leading to an improvement of 145.00 %. Unfortunately, the fill factor does not grow as the other parameters do. It

passes from 26.32 % for the REF-CELL to 22.70 % for the analogous cell with PbS. In order to achieve a higher efficiency for a fixed incident light power, the fill factor parameter is not as relevant as long as the short circuit current, the open circuit voltage or maximum power point suffer a higher increase. This is deduced looking into the equation [eq. 2]. Therefore, simply having better short-circuit current and open circuit voltage will lead to a better power conversion efficiency regardless the fill factor. This is just what has been found, the power conversion efficiency goes from 0.05 % for the reference cell to 0.12 % for that with PbS quantum dots. This represents a remarkably efficiency improvement of 140.00 %. Comparing Fig. 3a and 3b in darkness conditions, the PbS-CELL shows a low photovoltaic effect, not showing this effect the REF-CELL at short-circuit conditions. This slight effect could be due to a noisy background in terms of light, especially from the other heat instruments of the room. As the response to light is remarkably higher in the PbS-CELL, this background could be negligible for the reference cell.

While it is true that in absolute terms the efficiencies found for the devices are poor, it is necessary to remark that this could be due to the lack of any encapsulation, since it could lead to degradation and consequently low efficiencies, as it is widely known [16]. All devices were fabricated at room temperature without any control of the atmosphere. Thus, the goal of this study was to establish comparisons and not to fabricate devices with the highest efficiency.

The improvement of the electrical parameters of the hybrid solar cells fabricated embedding twofold stabilized PbS nanoparticles in blend active layer indicates that this easy fabrication procedure has combined good charge transfer, through shorter thiophenol ligand, with improved solubility from decanethiol.

4. Conclusions

PbS nanoparticles synthesized by a simple method using two stabilizing agents have shown good solubility in P3HT:PCBM polymer solution. TEM results show crystalline nanoparticles with an average size of 4.5 nm. The resulting compound has been used as the active layer for photovoltaic cells fabricated by spin-coating. Compared to cells based on bare P3HT:PCBM blend, hybrid photovoltaic cells exhibit an improvement of open voltage, short circuit, maximum power point and efficiency which suggests adequate electronic transport properties of the nanocomposite.

Conflicts of Interest

The authors declare that there is no conflicts of interest regarding the publication of this paper

Acknowledgments

This work has been partially supported by project MAT2012-37276 (Ministerio de Economía y Competitividad, Spain).

References

- [1] M. T. Dang, L. Hirsch, G. Wantz, *Adv. Mater.* **23**, 3597 (2011).
- [2] C. Goh, R. J. Kline, M. D. McGehee, E. N. Kadnikova, J. M. J. Fréchet, *Appl. Phys. Lett.* **86**, 122110 (2005).
- [3] L. J. A. Koster, V. D. Mihaileti, P. W. M. Blom, *Appl. Phys. Lett.* **88**, 093511 (2006).
- [4] C. M. Björström, A. Bernasik, J. Rysz, A. Budkowski, S. Nilsson, M. Svensson, M. R. Andersson, K. O Magnusson, E. Moons, *J. Phys-Condens. Mat.* **17**, L529 (2005).
- [5] S. E. Shaheen, C. J. Brabec, N. S. Sariciftci, F. Padinger, T. Fromherz, J. C. Hummelen, *Appl. Phys. Lett.* **78**, 841 (2001).
- [6] B. R. Saunders, M. L. Turner, *Adv. Colloid Interfac.* **138**, 1 (2008).
- [7] R. J. Ellingson, M. C. Beard, J. C. Johnson, P. Yu, O. I. Micic, A. J. Nozik, A. Shabaev, A. L. Efros, *Nano Lett.* **5**, 865 (2005).
- [8] J. C. Ferrer, A. Salinas-Castillo, J. L. Alonso, S. Fernández de Ávila, R. Mallavia, *Mat. Chem. Phys.* **122**, 459 (2010).
- [9] Y. Yin, A. P. Alivisatos, *Nature* **437**, 664 (2005).
- [10] N. Herron, Y. Wang, H. Eckert, *J. Am. Chem. Soc.* **112**, 1322 (1990).
- [11] P. R. Brown, D. Kim, R. R. Lunt, N. Zhao, M. G. Bawendi, J. C. Grossman, V. Bulovic, *ACS Nano.* **8**, 5863 (2014).
- [12] J. C. Ferrer, S. Fernández de Ávila, J. L. Alonso, *Proc. 10th Conference on Electron Devices*, 1 (2015).
- [13] J. L. Alonso, J. C. Ferrer, A. Salinas-Castillo, R. Mallavia, S. Fernández de Ávila, *Solid-State Electron* **54**, 1269 (2010).
- [14] D. W. Sievers, V. Shrotriya, Y. Yang, *J. Appl. Phys.* **100**, 114509 (2006).
- [15] F. W. Wise, *Acc. Chem. Res.* **33**, 773 (2000).
- [16] E. Vorosahzi, B. Verreet, T. Aernouts, P. Heremans, *Sol. Energy Mater. Sol. Cells* **95**, 1303 (2011).

*Corresponding author: j.l.alonso@umh.es